Which-way double-slit experiments and Born-rule violation

James Q. Quach*
ICFO - Institut de Ciències Fotòniques, Barcelona Institute of Science and Technology, 08860 Castelldefels, Spain
(Received 14 September 2016; published 24 April 2017)

In which-way double-slit experiments with perfect detectors, it is assumed that having a second detector at the slits is redundant because it will not change the interference pattern. We, however, show that if higher-order or nonclassical paths are accounted for, the presence of the second detector will have an effect on the interference pattern. Accounting for these nonclassical paths also means that the Sorkin parameter in triple-slit experiments is only an approximate measure of Born-rule violation. Using the difference between single and double which-way detectors, we give an alternative parameter which is an exact measure of Born-rule violation.

DOI: 10.1103/PhysRevA.95.042129

I. INTRODUCTION

The which-way double-slit experiment is used as the archetypal experiment to dramatically demonstrate the quantum weirdness of wave-particle duality and wave-function collapse: the explanation is that by merely knowing which slit the particle went through collapses the wave function, destroying the wave-like interference effects between the two slits. In the ideal case of perfect detectors, it is generally assumed that whether which-way detectors are placed at one slit or both will yield the same results. The reason for this is that a detection at one slit means that the particle is assumed to not have gone through the other slit. Now on the other hand, in the Feynman path integral formulation of quantum mechanics all possible paths between points contribute to the wave function; this even includes paths that go through one slit then the other as depicted in Fig. 1. The inclusion of these *nonclassical* or *high-order paths* provides corrections to the interference patterns.

The Born rule is a fundamental axiom of quantum mechanics. It states that if a quantum object is represented by a wave function $\psi(\mathbf{r},t)$, then the probability density of detecting it at position $\mathbf{r}$ and time t is given by the absolute square of the wave function [1],

$$P(\mathbf{r},t) = \psi^*(\mathbf{r},t)\psi(\mathbf{r},t) = |\psi(\mathbf{r},t)|^2. \quad (1)$$

Despite being a cornerstone of quantum mechanics, a direct test of the Born rule was not attempted until 2010 by Sinha *et al.* [2]. The test was a measure of the Sorkin parameter [3], which quantifies nonpairwise interference, in a triple-slit experiment. Since the exponent of the Born rule only allows for pairwise interference, a nonzero Sorkin parameter would suggest violation of the Born rule. If beyond-pairwise interference were indeed ever detected, it would likely lead to a modification of Schrödinger's equation, and may importantly provide a sign post for beyond standard model theories [4,5]. The Sinha *et al.* experiment, however, found the Sorkin parameter to be zero, within experimental error bounds, and concluded no Born-rule violation. Subsequent more precise measurements of the Sorkin parameter also came to the same conclusion [6–8]. Shortly after the Sinha *et al.* experiment, however, it was pointed out that underlying the Sorkin parameter was the assumption that the wave function in the multislit setup is simply the superposition of the individual wave functions of the constituent single-slit setups [9,10]. Strictly speaking this is an approximation, as first pointed out in Ref. [11]. Correcting this approximation by including nonclassical paths renders the Sorkin parameter nonzero, without violating the Born rule; in fact, in some regimes these corrections can be significant [9,10,12]. In a recent landmark experiment, a nonzero Sorkin parameter caused by nonclassical paths was indeed measured for the first time in the microwave regime [13]. The Sorkin parameter therefore is not an exact test of Born-rule violation. Given the success of quantum mechanics, any violation of the Born rule is expected to be small. Therefore for a parameter to be a useful measure of Born-rule violation, it is important that it is accurate to higher orders. One notes that alternatives to slit experiments, such as the single-spin experiment [14], may test the Born rule without the reliance on spatial interference.

Here we will show that by accounting for nonclassical paths, the which-way double-slit experiment with one and two which-way detectors will produce different interference patterns, contrary to commonly held assumptions. Making use of this difference, we give an alternative parameter that completely accounts for higher-order corrections, to exactly test the Born rule: the parameter will be exactly zero if the Born rule is not violated, nonzero otherwise. We first will consider the case of perfect detectors and then generalize to imperfect detectors.

II. PERFECT DETECTORS

A. Which-way double-slit experiment

Let us consider a double-slit experiment with two types of which-way detectors: one detects whether a particle has gone through slit A or B, the other detects that a particle has gone through one or both slits, but does not know which one. We will assume perfect detectors (Sec. III generalizes to imperfect detectors). Such detectors can be illustrated in a *gedanken* experiment, with light balls placed precariously in the slits to serve as the detectors (Fig. 1). In one type of detector a ball is placed in slit A, such that a particle entering the slit will cause it to fall into a tray. We look into the tray to reveal which slit the particle went through: if we see a ball in the tray then the particle went through slit A, if we do not see a ball, then the particle went through slit B. Implicit here is the

*quach.james@gmail.com

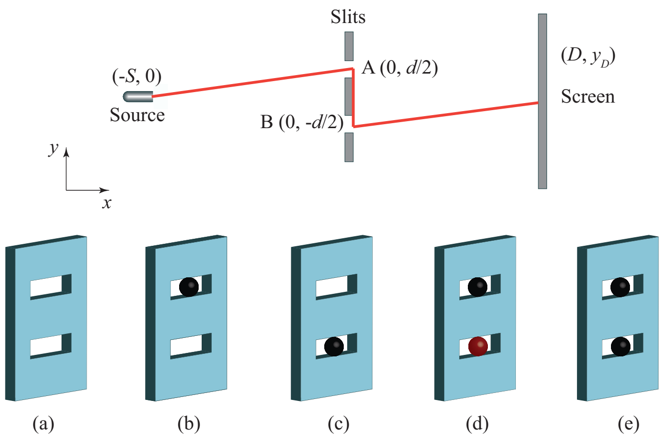

FIG. 1. Top: Side view of one of the myriad of nonclassical paths that enters both slits: the path enters slit A, makes an abrupt turn, briefly enters slit B, before hitting the detecting screen. Bottom: *gedanken* experiments with balls serving as detectors to illustrate different which-way detector setups. (a) setup 1: no which-way detectors, (b) setup 2: a type I which-way detector at slit A, (c) setup 3: a type I which-way detector at slit B, (d) setup 4: type I which-way detectors at slits A and B, (e) setup 5: a type II which-way detector.

assumption that we cannot directly view the ball until it hits the tray; in this sense the tray can be thought of as representing a signal amplifier. In another detector, indistinguishable balls are placed in each slit. In this case, peering into the tray we will see either one or two balls. One ball indicates that the particle had gone through one slit but it does not reveal which one, whereas two balls indicate that the particle had gone through both slits. We will call the former type I and latter type II which-way detectors. Such types of detectors have been realized in neutron [15] and molecular [16] interference setups, electrons in semiconductors [17], atomic double-pulse Ramsey interferometer experiments [18], inelastic electron holography [19], electron interferometers [20], and ion and electron beam nanofabrication [21].

If $\psi_{\rm A}$ represents the wave function from a single slit A and $\psi_{\rm B}$ from a single slit B, it is widely taught that the intensity or probability distribution in the double-slit experiment is $P_{\rm AB} = |\psi_{\rm A} + \psi_{\rm B}|^2$. The correction to this approximation can be quantified with the Feynman path integral formulation. In this formulation all paths between points are possible, even paths that are vastly different from classical paths (classical paths extremize the classical action). One of the myriad of nonclassical paths that enter both slits is depicted in Fig. 1. Because these types of paths enter both slits, they are not captured by the individual single-slit wave functions, $\psi_{\rm A}$ and $\psi_{\rm B}$. If we label the contribution from paths that go through both slits with $\psi_{\rm AB}$, the probability distribution for the double-slit experiment with no which-path detectors [Fig. 1(a): setup 1] is corrected to

$$P_{\rm AB} = |\psi_{\rm A} + \psi_{\rm B} + \psi_{\rm AB}|^2. \tag{2}$$

The higher-order corrections are typically small, but can be significant [9,10,12,13]. These corrections are not exclusive to the quantum mechanics, but are also present using Maxwell's equations as numerically calculated by Ref. [9]. Note that $\psi_{\rm A(B)}$ represents all paths that go through slit A (or B) only, including paths that go through that slit multiple times, and $\psi_{\rm AB}$ represents all paths that go through both slits including paths that enter the slits multiple times.

Now let us place a type I which-path detector at slit A [Fig. 1(b): setup 2]. Conventionally, a detection at slit A means that the particle did not go through slit B, otherwise the particle went through slit B, so that the probability density is $P_{D_{\rm A}} = |\psi_{\rm A}|^2 + |\psi_{\rm B}|^2$. This, however, does not account for nonclassical paths which can go through slits A and B. If one accounts for nonclassical paths, then a detection at slit A includes paths that only go through slit A as well as paths that go through slits A and B; since they are indistinguishable, we must sum both types of paths ($\psi_{\rm A} + \psi_{\rm AB}$). A nondetection at slit A means that the path must have gone through slit B only ($\psi_{\rm B}$). Thus the probability density when there is a type I which-path detector at slit A is

$$P_{D_{\rm A}} = |\psi_{\rm A} + \psi_{\rm AB}|^2 + |\psi_{\rm B}|^2; \tag{3}$$

and similarly when there is a which-way detector at slit B [Fig. 1(c): setup 3] the probability density is

$$P_{D_{\rm B}} = |\psi_{\rm B} + \psi_{\rm AB}|^2 + |\psi_{\rm A}|^2. \tag{4}$$

Now if we place a second type I detector at slit B, three types of paths are distinctly detected: paths that go through slit A ($\psi_{\rm A}$) or B ($\psi_{\rm B}$) only, and nonclassical paths that go through both before hitting the detection screen ($\psi_{\rm AB}$). In our *gedanken* experiment this is represented by placing two distinguishable (red and black) balls, one in each slit [Fig. 1(d): setup 4]. Looking into the tray we will see a black ball, a red ball, or both balls, to reveal that the particle had gone through slits A, B, or both, respectively. The probability density when there are type I detectors in both slits is therefore

$$P_{D_{\rm A}D_{\rm B}} = |\psi_{\rm A}|^2 + |\psi_{\rm B}|^2 + |\psi_{\rm AB}|^2. \tag{5}$$

When there is a type II which-path detector [Fig. 1(e): setup 5] one is not able to distinguish paths that contribute to $\psi_{\rm A}$ from $\psi_{\rm B}$. However, we can distinguish paths that went through one slit from paths that went through both slits before hitting the detecting screen. The probability density with a type II detector is

$$P_{D_{\rm AB}} = |\psi_{\rm A} + \psi_{\rm B}|^2 + |\psi_{\rm AB}|^2. \tag{6}$$

We would like now to quantify the difference in the probability distribution of the single (setup 2) and double (setup 4) which-way detector double-slit experiments. Let the source be at position $r_S = (-S,0)$, the screen detector at $r_D = (D, y_D)$, and slit centers are at $(0, \pm d/2)$ (Fig. 1). The slits have w width. The setup is symmetric in the z direction, which means we can ignore this component because it only introduces an irrelevant constant, effectively becoming a two-dimensional problem [10]. We assume a monochromatic point source and consider a duration much larger than the time of flight, so that the probability distribution at the screen detector can be quantified with the time-independent two-point propagator, which is attained by summing over all possible paths between $\mathbf{r}_1$ and $\mathbf{r}_2$,

$$K(\mathbf{r}_1,\mathbf{r}_2) = \int \mathcal{D}[\mathbf{x}(s)] \exp\left(ik \int ds\right), \tag{7}$$

where $\mathcal{D}[\mathbf{x}(s)]$ is the usual path integral measure of paths $\mathbf{x}(s)$ with contour length s. However, the problem of summing over all possible paths with the boundary conditions imposed by the slit plane is unwieldy and has yet to be exactly solved. Nevertheless, Sawant *et al.* [10] argue that a good approximation can be achieved by considering two types of paths: paths with straight trajectory segments from source to slit, then to detecting screen; and paths composing of straight trajectory segment from source to slit, then to another slit, before hitting the detection screen (Fig. 1). This conjecture has subsequently been supported with finite-difference time-domain simulations (FDTD) [12]. Following the convention of Sawant *et al.* we will call the former classical paths, and the latter nonclassical paths (as we have been doing). One notes that consideration of just the classical paths directly leads to Fresnel's theory of diffraction by a slit [22]. Using the following free propagator for straight paths [23]

$$K(\mathbf{r}_1,\mathbf{r}_1) = \frac{k}{2\pi i}\frac{e^{ik|\mathbf{r}_1-\mathbf{r}_2|}}{|\mathbf{r}_1-\mathbf{r}_2|}, \tag{8}$$

and the identity

$$K(\mathbf{r}_1,\mathbf{r}_3) = \int d\mathbf{r}_2 K(\mathbf{r}_1,\mathbf{r}_2)K(\mathbf{r}_2,\mathbf{r}_3), \tag{9}$$

the propagator for classical paths is

$$K_{\mathrm{P}}(\mathbf{r}_D,\mathbf{r}_S) = -\left(\frac{k}{2\pi i}\right)^2 \int dy \frac{e^{ik|l_1+l_2|}}{l_1 l_2}, \tag{10}$$

where $l_1 = (y^2+S^2)^{1/2}$, $l_2 = [(y_D-y)^2+D^2]^{1/2}$, and the integral runs over the width space of slit P. We will work in the Fraunhofer limit where the distance from the slit to the source and screen detector is much larger than the slit spacing, so that $l_1 \approx S + y^2/2S$ and $l_2 \approx D + (y_D-y)^2/2D$, giving ($\gamma \equiv \exp[ik(S+D)]/SD$) [10]

$$K_{\mathrm{P}}(\mathbf{r}_D,\mathbf{r}_S) \approx -\gamma\left(\frac{k}{2\pi i}\right)^2 \int dy\, e^{ik(\frac{y^2}{2S}+\frac{(y_D-y)^2}{2D})}. \tag{11}$$

The propagator for nonclassical paths is

$$K_{\mathrm{PQ}}(\mathbf{r}_D,\mathbf{r}_S) = \left(\frac{k}{2\pi i}\right)^3 \int dy_{\mathrm{P}}\, dy_{\mathrm{Q}} \frac{e^{ik|l_1+l_2+l_3|}}{l_1 l_2 l_3}, \tag{12}$$

where $l_1 = (y_{\mathrm{P}}^2+S^2)^{1/2}$, $l_2 = y_{\mathrm{Q}} - y_{\mathrm{P}}$, $l_3 = [(y_D-y)^2 + D^2]^{1/2}$, and the y_{P} (y_{Q}) integral runs over the width space of slit P (Q). In the Fraunhofer limit and under the stationary phase approximation [10],

$$K_{\mathrm{PQ}}(\mathbf{r}_D,\mathbf{r}_S) \approx \gamma i^{\frac{3}{2}}\left(\frac{k}{2\pi}\right)^{\frac{5}{2}} \int dy_{\mathrm{P}}\, dy_{\mathrm{Q}} |y_{\mathrm{Q}}-y_{\mathrm{P}}|^{-\frac{1}{2}} \times e^{ik(\frac{y_{\mathrm{P}}^2}{2S}+|y_{\mathrm{Q}}-y_{\mathrm{P}}|+\frac{(y_D-y)^2}{2D})}. \tag{13}$$

The Fraunhofer limit and stationary phase approximation introduce uncertainty on the order of $K \times 10^{-4}$ [10].

The contributions from nonclassical paths become more pronounced as the operating wavelength increases relative to slit spacing. The reason for this is that longer wavelengths mean more overlap between the single-slit wave functions, so that nonclassical paths which enter both slits are more likely. For this reason, the recent experiment which measured a nonzero Sorkin parameter worked in the microwave regime. Here as a case study we will consider the optical regime with the following parameters: photon source of $\lambda = 810$ nm wavelength, slit width $w = 500$ nm, interslit spacing of $d = 2000$ nm, and source and detector distances $S = D = 1$ mm.

For a point source at $\mathbf{r}_S$, $\psi(\mathbf{r}_D) = K(\mathbf{r}_D,\mathbf{r}_S)$, where $K(\mathbf{r}_D,\mathbf{r}_S)$ is the corresponding propagator from source to screen. Using Eqs. (11) and (13), Fig. 2(a) plots the intensity of the single which-way detector experiment (setup 2), $P_{D_{\mathrm{A}}}$; all plots are normalized to the maximum central intensity of the double-slit experiment, $P_{\mathrm{AB}}(0)$. ($P_{D_{\mathrm{B}}}$ is not shown because it is the same as Fig. 2(a) reflected about the y axis.) Figure 2(b) plots the intensity of the double which-way detector experiment (setup 4), $P_{D_{\mathrm{A}}D_{\mathrm{B}}}$. Figure 2(c) shows the difference in the interference pattern produced by the single and double which-way detector setups, $\Delta_1 \equiv P_{D_{\mathrm{A}}} - P_{D_{\mathrm{A}}D_{\mathrm{B}}}$.

The nonzero value of $\Delta_1 = \psi_{\mathrm{A}}\psi_{\mathrm{AB}}^* + \psi_{\mathrm{A}}^*\psi_{\mathrm{AB}}$ is the result of the interference between the single slit A and the nonclassical path wave functions. $\Delta_1/P_{\mathrm{AB}}(0)$ is on the order of 10^{-2}, which is much larger than the uncertainty introduced by the Fraunhofer limit and stationary phase approximation. In the optical regime, the Sinha *et al.* experiment achieved intensity accuracies of order 10^{-2} normalized to the expected two-path interference, and subsequent experiments with multipath interferometers [6,8] have claimed accuracies of at least an order of magnitude better. If the same sort of accuracy can be achieved in double-slit experiments with which-way detectors, the effects of the second which-way detector on the interference pattern due to nonclassical paths should be detectable.

For completeness we have also plotted the intensities of P_{AB} and $P_{D_{\mathrm{AB}}}$, and their difference, Δ_2, in Figs. 2(d)–2(f). The nonzero value of $\Delta_2 = (\psi_{\mathrm{A}}+\psi_{\mathrm{B}})\psi_{\mathrm{AB}}^* + (\psi_{\mathrm{A}}+\psi_{\mathrm{B}})^*\psi_{\mathrm{AB}}$ is the result of the interference between the classical and nonclassical path wave functions of the double slits.

B. Born-rule violation

The Sorkin parameter for the triple-slit experiment is defined as

$$\mathcal{I}_{\mathrm{ABC}} \equiv \mathcal{P}_{\mathrm{ABC}} - \mathcal{P}_{\mathrm{AB}} - \mathcal{P}_{\mathrm{AC}} - \mathcal{P}_{\mathrm{BC}} + \mathcal{P}_{\mathrm{A}} + \mathcal{P}_{\mathrm{B}} + \mathcal{P}_{\mathrm{C}}, \tag{14}$$

where $\mathcal{P}_{\mathrm{ABC}}$ is the probability of detection when all three slits (A, B, C) are open, $\mathcal{P}_{\mathrm{AB}}$ is the probability of detection when two slits (A, B) are open, and so on. If one assumes that the probabilities are simply given by the linear superposition of the individual wave functions of the constituent single-slit setups ($\mathcal{P}_{\mathrm{ABC}} = |\psi_{\mathrm{A}}+\psi_{\mathrm{B}}+\psi_{\mathrm{C}}|^2$, $\mathcal{P}_{\mathrm{AB}} = |\psi_{\mathrm{A}}+\psi_{\mathrm{B}}|^2$, and so on), then by rewriting probabilities in Eq. (14) in terms of wave functions, it can be shown that $\mathcal{I}_{\mathrm{ABC}} = 0$ if the Born rule is correct. The proposed advantage of using the Sorkin parameter to experimentally test the Born rule is that one does not need to know the theoretical values of these probabilities, one need only measure them.

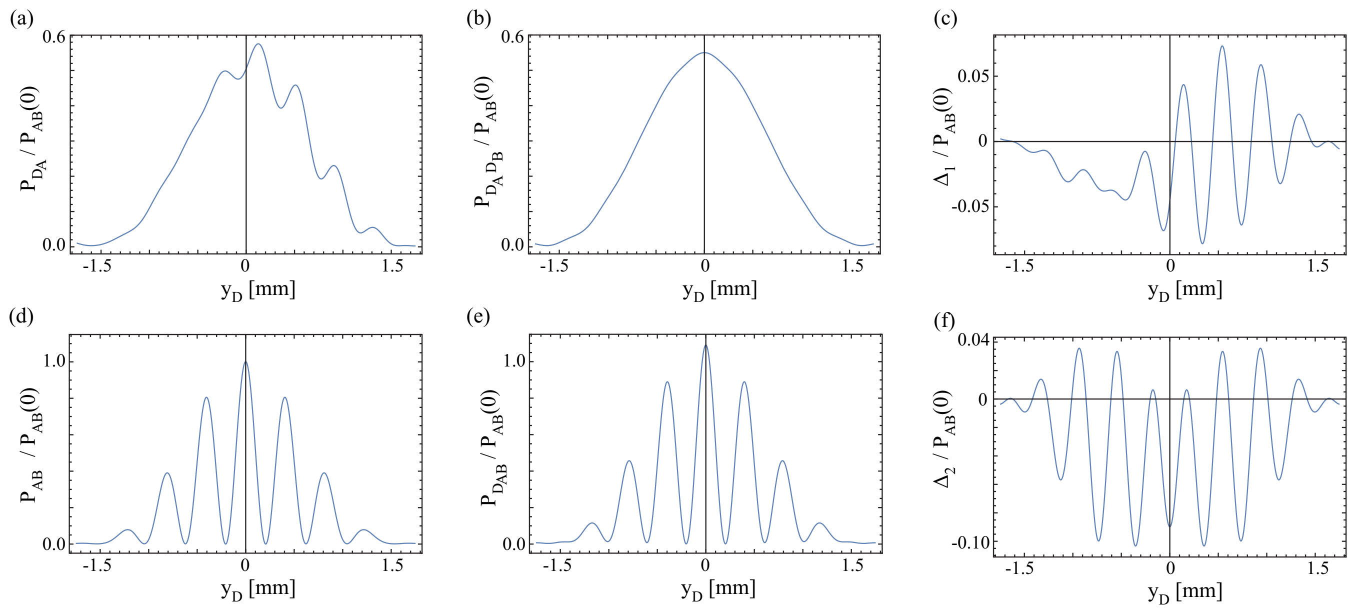

FIG. 2. (a) Normalized intensity of the single type I which-way detector experiment (setup 2). (b) Normalized intensity of the double type I which-way detector experiment (setup 4). (c) Difference in the interference pattern produced by the single and double type I which-way detector experiments, $\Delta_1 \equiv P_{D_A} - P_{D_A D_B}$. (d) Normalized intensity of the double-slit experiment without which-way detectors (setup 1). (e) Normalized intensity of the type II which-way detector experiment (setup 5). (e) Difference in the interference pattern between setup 1 and setup 5, $\Delta_2 \equiv P_{AB} - P_{D_{AB}}$. Parameters: photon source of $\lambda = 810$ nm wavelength, slit width $w = 500$ nm, interslit spacing of $d = 2000$ nm, and source and detector distances $S = D = 1$ mm. All plots are normalized to the maximum central intensity of the double-slit experiment, $P_{AB}(0)$.

If one accounts for nonclassical paths, the probability of detection must be corrected to $\mathcal{P}_{ABC} = |\psi_A + \psi_B + \psi_C + \psi_{ABC}|^2$, where ψ_{ABC} is the wave function made up of nonclassical paths when slits A, B, and C are open, which are not accounted for by single-slit wave functions ψ_A, ψ_B, ψ_C. Similar corrections are required for two slits, e.g., $\mathcal{P}_{AB} = |\psi_A + \psi_B + \psi_{AB}|^2$. The inclusion of these corrections mean that $I_{ABC} \neq 0$. This was first noted by De Raedt *et al.* [9]. Because the interference pattern of the triple-slit experiment can be described classically, Raedt *et al.* solved Maxwell's equation with FDTD simulations to show that the linear single-slit wave-function superposition assumption underlying the Sorkin parameter was not correct; therefore $I_{ABC} \neq 0$ does not immediately signal Born-rule violation.

In principle one may theoretically calculate this nonzero value of I_{ABC} with the higher-order corrections. In practice, however, there are an infinite number of nonclassical paths and an exact calculation is currently impossible (work in this field has produced approximate closed-form solutions [12]). Having to theoretically calculate probabilities negates the main benefit of using the Sorkin parameter, which is to test the Born rule without the need for such calculations.

Furthermore there are regimes where nonclassical paths can have significant contributions, as shown in Fig. 2, and therefore produce relatively large values of the Sorkin parameter even though the Born rule has not been violated. Here we introduce an alternative parameter which will produce exactly zero in all regimes when the Born rule is not violated.

The Sorkin parameter can be generalized to systems with three and more slits, but not two slits. The reason for this is that $\mathcal{I}_{AB} \equiv \mathcal{P}_{AB} - \mathcal{P}_A - \mathcal{P}_B \neq 0$ even if one ignores the nonclassical paths. This is why the triple-slit experiment is the simplest setup to test the Born rule with the Sorkin parameter. However, if one adds which-way detectors, double-slit experiments can be used to exactly test the Born rule. In particular we introduce the following parameter as an exact test of the Born rule:

$$I_{AB} \equiv P_{AB} - P_{D_A} - P_{D_B} - P_{D_{AB}} + 2P_{D_A D_B}. \tag{15}$$

Substitution of Eqs. (2)–(6) into Eq. (15) shows that $I_{AB} = 0$. Like the Sorkin parameter, I_{AB} subtracts from P_{AB} all possible combinations of pairwise interaction terms yielding $I_{AB} = 0$ if the Born rule holds; if the probability of detection is anything other than the absolute square of the wave function, then $I_{AB} \neq 0$ in general. Different from the Sorkin parameter, however, I_{AB} exactly accounts for the higher-order corrections to all orders. This allows an exact direct test of the Born rule, limited only to experimental uncertainty.

Specifically, the experiment to test the Born rule will involve repeating the double-slit experiments five times, each time the only thing to be changed is the which-path detector configuration, to get values for $P_{AB}, P_{D_A}, P_{D_B}, P_{D_{AB}}$, and $P_{D_A D_B}$. One may then measure I_{AB} using Eq. (15): any value other than $I_{AB} = 0$ signals Born-rule violation.

III. IMPERFECT DETECTORS

In practice, detectors are imperfect, whether by design or because of technical limitations. Which-way detectors with controllable efficiency have been used in experiments to reveal the quantum-classical boundary [18,20,21]. Unlike perfect detectors, imperfect detectors introduce detection efficiency as additional parameters. Here we will consider the case of detectors with the same efficiency. For a case study we will use the parameters set in Sec. II.

To study the double-slit experiment with imperfect detectors we write down the basis-independent representation of the wave functions in the previous section as $|\psi_{\mathrm{A}}\rangle$, $|\psi_{\mathrm{B}}\rangle$, and $|\psi_{\mathrm{AB}}\rangle$ (we will project to the position basis in the end). When there are no detectors the state of the particle at the detection screen is

$$|\psi\rangle = |\psi_{\mathrm{A}}\rangle + |\psi_{\mathrm{B}}\rangle + |\psi_{\mathrm{AB}}\rangle. \tag{16}$$

In the presence of detectors, the particle becomes entangled with the detector as it pass through the slits. We denote the normalized triggered state of a type I detector at slit A (setup 2) as $|D_{\mathrm{A}}\rangle$ and the normalized untriggered state as $|0\rangle$. In terms of the *gedanken* experiment, these states of the detector are represented by 1 and 0 balls in the tray, respectively. The state of the system after the particle passes through the slit plane is

$$|\phi_{D_{\mathrm{A}}}\rangle = (|\psi_{\mathrm{A}}\rangle + |\psi_{\mathrm{AB}}\rangle)|1_{\mathrm{A}}\rangle + |\psi_{\mathrm{B}}\rangle|0\rangle. \tag{17}$$

We are only interested in the probability of detection of the particle at the detection screen, so we trace out the detector states from the density matrix obtained from the pure state of Eq. (17). We project this reduced density matrix onto the position basis to get the probability distribution

$$P'_{D_{\mathrm{A}}} = |\psi_{\mathrm{A}} + \psi_{\mathrm{AB}}|^2 + |\psi_{\mathrm{B}}|^2 + 2\mathrm{Re}[(\psi_{\mathrm{A}} + \psi_{\mathrm{AB}})^*\psi_{\mathrm{B}}]\langle 0|D_{\mathrm{A}}\rangle. \tag{18}$$

$\langle 0|D_{\mathrm{A}}\rangle$ is the amount of overlap between the triggered and untriggered detector states, which determines the level of interference in the probability distribution. When these states are orthogonal, one retrieves the perfect detector probability distribution of Eq. (3). An operative understanding of the overlap term is made clear by setting $\langle 0|D_{\mathrm{A}}\rangle = 1 - n$, where $0 \leqslant n \leqslant 1$, and rewriting Eq. (18) as

$$P'_{D_{\mathrm{A}}} = nP_{D_{\mathrm{A}}} + (1-n)P_{\mathrm{AB}}. \tag{19}$$

From Eq. (19) we can interpret n as the efficiency of the detector at slit A: the detector will detect an event with efficiency n and when it does, the probability distribution is $P_{D_{\mathrm{A}}}$; and the detector will miss an event with efficiency $1 - n$ and when it does, the probability distribution is P_{AB}. Similarly for a detector at slit B only, one gets

$$P'_{D_{\mathrm{B}}} = nP_{D_{\mathrm{B}}} + (1-n)P_{\mathrm{AB}}. \tag{20}$$

For a type I detector at each of the slits (setup 3), we denote the normalized states of the detector system as $|D_{\mathrm{A}}\rangle$, $|D_{\mathrm{B}}\rangle$, and $|D_{\mathrm{A}}D_{\mathrm{B}}\rangle$ (representing the black, red, and black and red ball states in the *gedanken* experiment). The state of the system after the slit plane is

$$|\phi_{D_{\mathrm{A}}D_{\mathrm{B}}}\rangle = |\psi_{\mathrm{A}}\rangle|D_{\mathrm{A}}\rangle + |\psi_{\mathrm{B}}\rangle|D_{\mathrm{B}}\rangle + |\psi_{\mathrm{AB}}\rangle|D_{\mathrm{A}}D_{\mathrm{B}}\rangle. \tag{21}$$

The corresponding probability distribution is

$$P'_{D_{\mathrm{A}}D_{\mathrm{B}}} = |\psi_{\mathrm{A}}|^2 + |\psi_{\mathrm{B}}|^2 + |\psi_{\mathrm{AB}}|^2 + 2\mathrm{Re}[\psi_{\mathrm{A}}^*\psi_{\mathrm{B}}\langle D_{\mathrm{B}}|D_{\mathrm{A}}\rangle + \psi_{\mathrm{A}}^*\psi_{\mathrm{AB}}\langle D_{\mathrm{A}}D_{\mathrm{B}}|D_{\mathrm{A}}\rangle + \psi_{\mathrm{B}}^*\psi_{\mathrm{AB}}\langle D_{\mathrm{A}}D_{\mathrm{B}}|D_{\mathrm{B}}\rangle]. \tag{22}$$

Equation (22) is a general representation of the probability distribution. Let us consider the case where $\langle D_{\mathrm{A}}D_{\mathrm{B}}|D_{\mathrm{A}}\rangle = \langle D_{\mathrm{A}}D_{\mathrm{B}}|D_{\mathrm{B}}\rangle = 1 - n$ and $\langle D_{\mathrm{B}}|D_{\mathrm{A}}\rangle = (1-n)^2$. This yields

$$P'_{D_{\mathrm{A}}D_{\mathrm{B}}} = n^2P_{D_{\mathrm{A}}D_{\mathrm{B}}} + n(1-n)(P_{D_{\mathrm{A}}} + P_{D_{\mathrm{B}}}) + (1-n)^2P_{\mathrm{AB}}. \tag{23}$$

Our choice of detector-state overlaps can thus be interpreted as the result of two n-efficient, type I which-way detectors at slits A and B, with n^2 probability that both detectors can detect an event, $n(1-n)$ probability that one detector can detect an event and the other does not, and $(1-n)^2$ probability that both detectors missed an event.

A comparison of Eqs. (18) and (22) shows that even if nonclassical paths are neglected (i.e., $\psi_{\mathrm{AB}} = 0$), the presence of a second which-way detector can have an effect on the probability distribution when the detectors are imperfect; formally the difference results from the fact that $\langle 0|D_{\mathrm{A}}\rangle \neq \langle D_{\mathrm{B}}|D_{\mathrm{A}}\rangle$ in general. Note that unlike Eqs. (19) and (20), Eq. (23) is implementation specific, dependent on the form of the overlap of detector states.

For the type II detector (setup 4), we denote the normalized states of the detector system as $|D_1\rangle$ and $|D_2\rangle$ (representing the one and two indistinguishable-ball states in the *gedanken* experiment). The state of the system after the slit plane is

$$|\phi_{D_{\mathrm{AB}}}\rangle = (|\psi_{\mathrm{A}}\rangle + |\psi_{\mathrm{B}}\rangle)|D_1\rangle + |\psi_{\mathrm{AB}}\rangle|D_2\rangle. \tag{24}$$

The corresponding probability distribution is

$$P'_{D_{\mathrm{AB}}} = |\psi_{\mathrm{A}}|^2 + |\psi_{\mathrm{B}}|^2 + |\psi_{\mathrm{AB}}|^2 + 2\mathrm{Re}(\psi_{\mathrm{A}}^*\psi_{\mathrm{B}}) + 2\mathrm{Re}(\psi_{\mathrm{A}}^*\psi_{\mathrm{AB}} + \psi_{\mathrm{B}}^*\psi_{\mathrm{AB}})\langle D_2|D_1\rangle. \tag{25}$$

$\langle D_2|D_1\rangle$ gives the amount of overlap between the one and two indistinguishable-ball states. When these states are orthogonal, we can be sure that the particle has passed through one or two slits. Conversely, when the states completely overlap we have no information on whether the particle has passed through one or two slits, which is equivalent to having no detectors. In between these two extremes, the detector states partially overlap and we have an imperfect, type II which-way detector. Setting $\langle D_2|D_1\rangle = 1 - n$, Eq. (25) can be rewritten as

$$P'_{D_{\mathrm{AB}}} = nP_{D_{\mathrm{AB}}} + (1-n)P_{\mathrm{AB}}. \tag{26}$$

Figures 3(a)–3(d) plots $P'_{D_{\mathrm{A}}}$ (solid line) and $P'_{D_{\mathrm{A}}D_{\mathrm{B}}}$ (dashed line) for $n = 0.25,0.5,0.75,1$ under the parameters set in Fig. 2. As the efficiency increases there is a transition from classical wave-like interference to corpuscular quantum behavior due to which-way detector observation. The presence of a second which-way detector increases the efficiency of detection, thereby seeing an earlier transition to corpuscular behavior.

For comparison we also plot $P'_{D_{\mathrm{A}}}$ (solid line) and $P'_{D_{\mathrm{A}}D_{\mathrm{B}}}$ (dashed line) when the higher-order contributions are ignored (i.e., $\psi_{\mathrm{AB}} = 0$) in Figs. 3(e)–3(h). As detector error is eliminated, detection efficiency is eliminated as a parameter which can distinguish the presence of a second detector. If higher-order contributions are neglected, then there is no difference between having one or two perfect detectors, as shown in Fig. 3(h). In contrast, if one accounts for higher-order contributions, even as detector error is eliminated, the presence of a second detector cannot be made redundant [Fig. 3(d)], as discussed in the Sec. II.

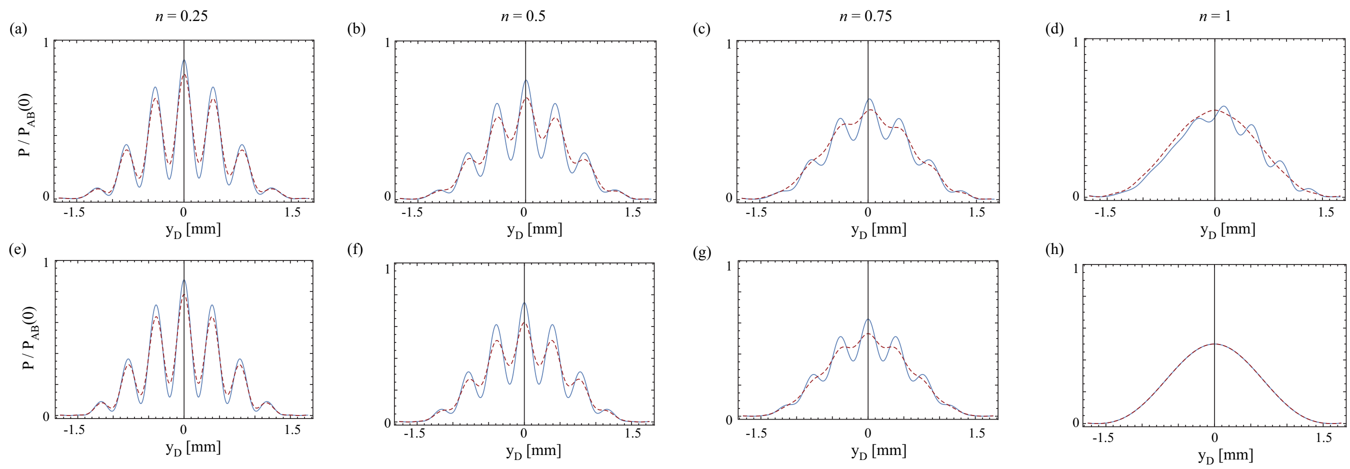

FIG. 3. Comparative plots of single (solid blue line) and double (dashed red line) which-way detectors. (a)–(d) P'_{D_A} and $P'_{D_A D_B}$ with higher-order contributions for detector efficiencies $n = 0.25, 0.5, 0.75, 1$. (e)–(f) P'_{D_A} and $P'_{D_A D_B}$ without higher-order contributions. As the efficiency increases there is a transition from classical wave-like interference to corpuscular quantum behavior. Parameter values follow Fig. 2.

As which-way detectors are not perfect, in practice it is more likely that $P'_{D_A}, P'_{D_B}, P'_{D_A D_B}$, and $P'_{D_{AB}}$ will be the measured quantities. Therefore, by simultaneously solving Eqs. (19), (20), (23), and (26), we write here the perfect ($n = 1$) probability distributions as functions of the imperfect probability distributions ($0 < n < 1$):

$$P_{D_A} = \frac{P'_{D_A} - (1-n)P_{AB}}{n}, \tag{27}$$

$$P_{D_B} = \frac{P'_{D_B} - (1-n)P_{AB}}{n}, \tag{28}$$

$$P_{D_A D_B} = \frac{P'_{D_A D_B} + (1-n)^2 P_{AB} - (1-n)\left(P'_{D_A} + P'_{D_B}\right)}{n^2}, \tag{29}$$

$$P_{D_{AB}} = \frac{P'_{D_{AB}} - (1-n)P_{AB}}{n}, \tag{30}$$

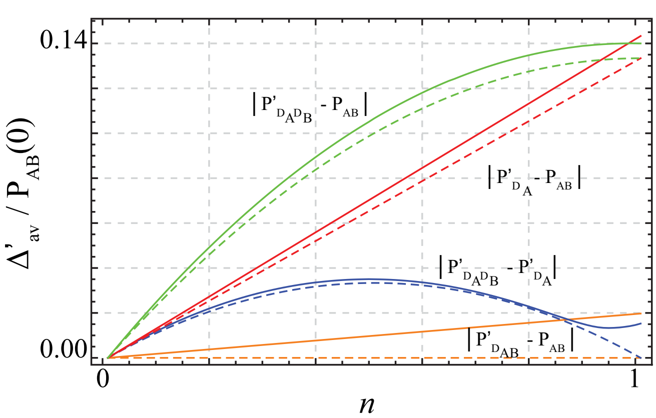

FIG. 4. Average absolute difference in probability distributions as function of which-way detector efficiency. The solid (dashed) line plots the average difference in probability distribution Δ'_{av}, with (without) higher-order contributions, between $y_1 = -1.75$ mm and $y_2 = 1.75$ mm. Other parameter values follow Fig. 2.

Substitution of Eqs. (27)–(30) into Eq. (15) gives the parameter to test for Born-rule violation in terms of the measured probability distributions with inefficient which-way detectors. Using this substitution one may then test the Born rule with inefficient detectors. Retrieving the perfect probability distributions from the imperfect ones, however, requires resolutions that can distinguish the different imperfect probability distributions.

Figure 4 plots the average absolute difference in the probability distribution as a function of detector efficiency for the various probability functions of Eqs. (19), (20), (23), and (26), with higher-order contributions (solid line) and without higher-order contributions (dashed line),

$$\Delta'_{av} = \frac{1}{y_2 - y_1} \int_{y_1}^{y_2} |P'_P - P'_Q| dy. \tag{31}$$

Overall the lower the efficiency of the detectors, the harder it is to distinguish the different imperfect probability distributions, with the difference between P'_{D_A} and $P'_{D_A D_B}$ (solid blue line), and $P_{D_{AB}}$ and P'_{AB} (solid orange line) being the most difficult to observe. [Note that Fig. (3) corresponds to the blue lines in Fig. (4).] Under the experimental parameters used in Fig. (2), if one were to achieve an accuracy of 10^{-2} in the measurement of the probability distributions (as achieved by the Sinha *et al.* experiment [2]), then Fig. 4 shows that the which-way detector efficiency required to distinguish the different imperfect probability distributions would need to be greater than 50%.

IV. CONCLUSION

We have shown that the inclusion of higher-order or nonclassical paths will lead to different interference patterns for which-way double-slit experiments with one and two which-way detectors. These differences should be measurable in regimes where the operating wavelength is commensurate to or larger than slit spacing. Previously, direct tests of the

Born rule have been triple-slit experiments measuring the Sorkin parameter. The Sorkin parameter, however, is only an approximate test of the Born rule, and can only be applied in regimes where the operating wavelength is much smaller than slit spacing. By explicitly accounting for higher-order correction, we have given an alternative parameter which is an exact test of the Born rule for all wavelengths and slit spacing. This should open up a new suite of experiments based on which-path double-slit experiments, to test the Born rule to accuracies limited only by experimental uncertainties and not theoretical ones.

ACKNOWLEDGMENTS

The author thanks M. Lajkó, A. Celi, C.-H. Su, and S. Quach for discussions and checking the manuscript. This work was financially supported by the European Commission's Marie Curie Actions for Co-funding of Regional, National and International Programmes (COFUND), the Spanish Ministry of Economy and Competitiveness (MINECO), Fundacio Privada Cellex, Spanish Ministerio de Economía y Competitividad grants (Severo Ochoa SEV-2015-0522 and FOQUS FIS2013-46768-P), and Generalitat de Catalunya (SGR 874).

[1] M. Born, Quantenmechanik der stoßvorgänge, Z. Phys. **38**, 803 (1926).

[2] U. Sinha, C. Couteau, T. Jennewein, R. Laflamme, and G. Weihs, Ruling out multi-order interference in quantum mechanics, Science **329**, 418 (2010).

[3] R. D. Sorkin, Quantum mechanics as quantum measure theory, Mod. Phys. Lett. A **09**, 3119 (1994).

[4] H. Barnum, M. P. Müller, and C. Ududec, Higher-order interference and single-system postulates characterizing quantum theory, New J. Phys. **16**, 123029 (2014).

[5] C. M. Lee and J. H. Selby, Higher-order interference in extensions of quantum theory, Found. Phys. **47**, 89 (2017).

[6] I. Söllner, B. Gschösser, P. Mai, B. Pressl, Z. Vörös, and G. Weihs, Testing Born's rule in quantum mechanics for three mutually exclusive events, Found. Phys. **42**, 742 (2012).

[7] D. K. Park, O. Moussa, and R. Laflamme, Three path interference using nuclear magnetic resonance: A test of the consistency of Born's rule, New J. Phys. **14**, 113025 (2012).

[8] T. Kauten, R. Keil, T. Kaufmann, B. Pressl, Č. Brukner, and G. Weihs, Obtaining tight bounds on higher-order interferences with a 5-path interferometer, New J. Phys. **19**, 033017 (2017).

[9] H. De Raedt, K. Michielsen, and K. Hess, Analysis of multipath interference in three-slit experiments, Phys. Rev. A **85**, 012101 (2012).

[10] R. Sawant, J. Samuel, A. Sinha, S. Sinha, and U. Sinha, Nonclassical Paths in Quantum Interference Experiments, Phys. Rev. Lett. **113**, 120406 (2014).

[11] H. Yabuki, Feynman path integrals in the young double-slit experiment, Int. J. Theor. Phys. **25**, 159 (1986).

[12] A. Sinha, A. H. Vijay, and U. Sinha, On the superposition principle in interference experiments, Sci. Rep. **5**, 10304 (2015).

[13] G. Rengaraj, U. Prathwiraj, S. N. Sahoo, R. Somashekhar, and U. Sinha, Measuring the deviation from the superposition principle in interference experiments, arXiv:1610.09143.

[14] F. Jin, Y. Liu, J. Geng, P. Huang, W. Ma, M. Shi, C.-K. Duan, F. Shi, X. Rong, and J. Du, Experimental test of Born's rule by inspecting third-order quantum interference on a single spin in solids, Phys. Rev. A **95**, 012107 (2017).

[15] J. Summhammer, H. Rauch, and D. Tuppinger, Stochastic and deterministic absorption in neutron-interference experiments, Phys. Rev. A **36**, 4447 (1987).

[16] A. D. Cronin, J. Schmiedmayer, and D. E. Pritchard, Optics and interferometry with atoms and molecules, Rev. Mod. Phys. **81**, 1051 (2009).

[17] I. L. Aleiner, N. S. Wingreen, and Y. Meir, Dephasing and the Orthogonality Catastrophe in Tunneling Through a Quantum Dot: The "Which Path?" Interferometer, Phys. Rev. Lett. **79**, 3740 (1997).

[18] P. Bertet, S. Osnaghi, A. Rauschenbeutel, G. Nogues, A. Auffeves, M. Brune, J. M. Raimond, and S. Haroche, A complementarity experiment with an interferometer at the quantum-classical boundary, Nature **411**, 166 (2001).

[19] P. L. Potapov, H. Lichte, J. Verbeeck, and D. Van Dyck, Experiments on inelastic electron holography, Ultramicroscopy **106**, 1012 (2006).

[20] P. Sonnentag and F. Hasselbach, Measurement of Decoherence of Electron Waves and Visualization of the Quantum-Classical Transition, Phys. Rev. Lett. **98**, 200402 (2007).

[21] S. Frabboni, G. C. Gazzadi, and G. Pozzi, Ion and electron beam nanofabrication of the which-way double-slit experiment in a transmission electron microscope, Appl. Phys. Lett. **97**, 263101 (2010).

[22] P. B. S. Kumar and G. S. Ranganath, Geometrical theory of diffraction, Pramana **37**, 457 (1991).

[23] L. D. Landau and E. M. Lifshitz, *The Classical Theory of Fields*, 4th ed. (Pergamon, Oxford, 1975), Vol. 2, p. 156.